An *ab initio* and DFT study of homolytic substitution reactions of acyl radicals at sulfur, selenium, and tellurium†‡

Sonia M. Horvat*[ab] and Carl H. Schiesser[ab]

Received (in Victoria, Australia) 16th February 2010, Accepted 27th April 2010
DOI: 10.1039/c0nj00125b

Ab initio calculations using the 6-311G**, cc-pVDZ, aug-cc-pVDZ, and (valence) double-ζ pseudopotential (DZP) basis sets, with (MP2, ROMP2, QCISD, CCSD(T)) and without (HF) the inclusion of electron correlation, and density functional (BHandHLYP and B3LYP) calculations predict that homolytic substitution reactions of acetyl radicals at the sulfur, selenium and tellurium atoms in dimethyl sulfide, dimethyl selenide, and dimethyl telluride adopt an almost collinear arrangement of attacking and leaving radicals at the chalcogen atom. Energy barriers ($\Delta E^{\ddagger}$) for these reactions range from 76.5 (attack at S, BHandHLYP/6-311G**) to 35.5 kJ mol^{-1} (attack at Te, BHandHLYP/DZP). While the calculated energy barriers for the forward and reverse energy barriers for substitution of acetyl radical at the sulfur atom are comparable, the reverse reactions are favoured by 3–14 kJ mol^{-1} for attack at selenium and by 20–25 kJ mol^{-1} for attack at tellurium.

Introduction

Homolytic addition and substitution reactions play central roles in organic chemistry and are now considered effective methods for formation of carbon–carbon and carbon–heteroatom bonds.[1,2] Homolytic substitution chemistry is particularly effective for the preparation of chalcogen-containing rings and examples that illustrate the formation of benzothiophenes (**1**), selenophenes (**2**) and benzotellurophenes (**3**) are provided in Scheme 1.[3] While acyl radicals have been extensively used in homolytic addition,[4] there are many fewer examples of their use in substitution chemistry; one example is provided in Scheme 2 in which Ryu and co-workers showed that acyl radical **4** undergoes ring closure at sulfur with expulsion of a *tert*-butyl radical to afford the thiolactone **5**, with a rate constant for cyclization of approximately 7.5×10^3 s^{-1} at 25 °C.[5] In comparison, the analogous cyclization involving an alkyl radical is significantly slower, with the rate constant determined to be 2.7×10^2 s^{-1} at 25 °C.[6] Although the mechanism of inter- and intramolecular homolytic substitution of alkyl radicals at heteroatoms has been largely elucidated,[7] relatively little is known about these types of reactions involving acyl radicals.

It is generally agreed that homolytic substitution by an attacking radical (R) at a main-group heteroatom (Y) involves the approach of the radical along a trajectory opposite to the leaving group (Z). Possible pathways for this chemistry to take place include a concerted process where the attacking and leaving radical adopt a collinear (or nearly so) arrangement

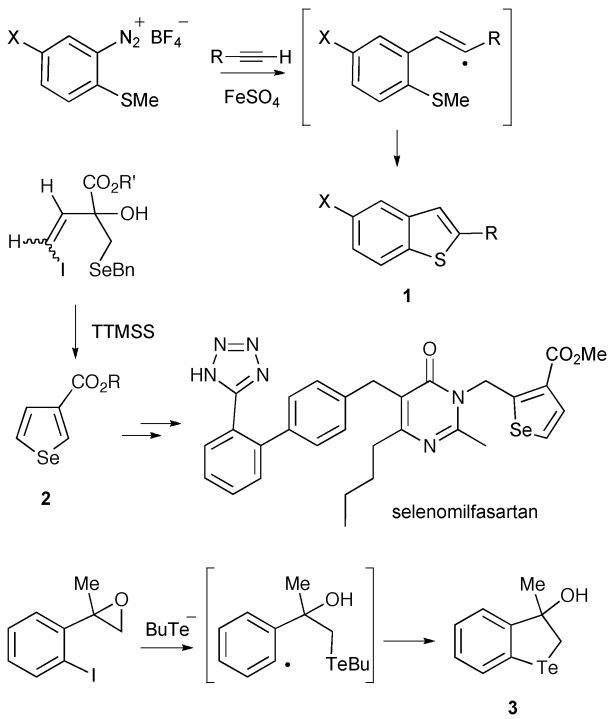

Scheme 1

(**6**), resulting in Walden inversion, and the involvement of a hypervalent intermediate (**7**) which may or may not undergo pseudorotation prior to dissociation.[1,8]

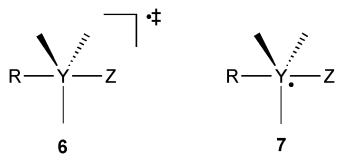

6 **7**

Work in our laboratories has been directed toward the understanding and utilization of free-radical homolytic

[a] *School of Chemistry, The University of Melbourne, Victoria, Australia. E-mail: shorvat@unimelb.edu.au*
[b] *Bio21 Molecular Science and Biotechnology Institute, The University of Melbourne, Victoria, Australia*

† This article is part of a themed issue on Main Group chemistry.
‡ Electronic supplementary information (ESI) available: Table S1 and optimized geometries and energies for all transition state structures. See DOI: 10.1039/c0nj00125b

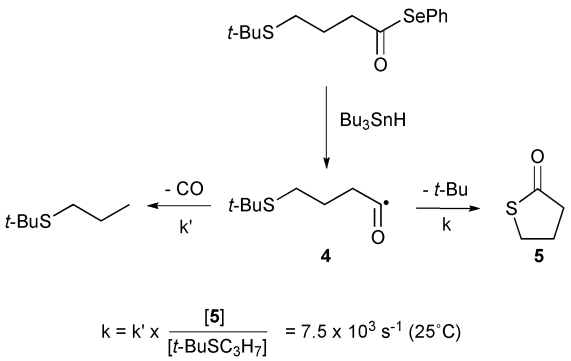

Scheme 2 Rate constant for intermolecular S_H2 at sulfur by an acyl radical.

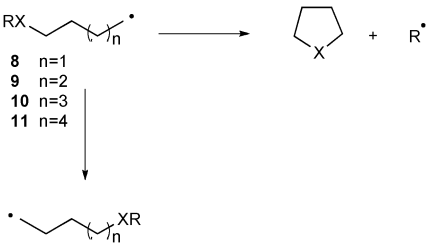

Scheme 3

substitution chemistry,[9–11] and as such we have published several *ab initio* and DFT studies with the aim of increasing our understanding of the factors that affect and control the mechanism of radical reactions involving main-group heteroatoms.[8–10] While our mechanistic studies involving the chalcogens suggest that homolytic substitutions by alkyl radicals at sulfur and selenium proceed *via* smooth transition states and the analogous reactions involving tellurium are predicted to involve hypervalent intermediates,[9,12] substitution reactions by silyl, germyl, and stannyl radicals at the analogous alkylchalcogenides do not involve intermediates.[9] In addition, intramolecular homolytic substitution at the chalcogen atoms in radicals **8–11** is calculated to proceed preferentially by degenerate translocation of the chalcogen-containing moiety for radicals **10** and **11**, and with ring closure in the case of **8** and **9** (Scheme 3).[12]

As part of our ongoing interest in homolytic substitution chemistry involving the main group heteroatoms and in order to provide further insight into the mechanistic details of homolytic substitution of acyl radicals at higher heteroatoms we began to explore the chemistry of acetyl radical with dimethyl sulfide, dimethyl selenide, and dimethyl telluride using computational techniques.

Computational methods

Ab initio and Density Functional Theory (DFT) calculations were carried out using the Gaussian 03 program.[13] Geometry optimisations were performed with standard gradient techniques at HF, MP2, B3LYP and BHandHLYP levels of theory, using restricted and unrestricted methods for closed- and open-shell systems, respectively.[14] Basis sets available in Gaussian 03 were used, as well as the (valence) double-ζ pseudopotential basis sets of Hay and Wadt[15] supplemented with a single set of *d*-type polarization functions for the heteroatom in this study (exponents $d(\zeta)_{Te} = 0.252$),[16] together with the double-ζ all-electron basis sets of Dunning and Hay[17] with additional set of polarization functions (exponents $d(\zeta)_C = 0.75$, $d(\zeta)_O = 0.85$ and $p(\zeta)_H = 1.00$) were used for C, O and H. We refer to this basis set as DZP throughout this work. In previous work, results generated using DZP proved to be very similar to those obtained using 6-311G(d,p) for reactions involving silicon and chlorine.[10b,c] All ground and transition states were verified by vibrational frequency analysis. Further single-point ROMP2, QCISD and CCSD(T) calculations were performed on selected MP2, B3LYP and BHandHLYP optimized structures as detailed in Tables 2 and 4. When correlated methods were used, calculations were carried out by using the frozen core approximation. Values of $\langle s^2 \rangle$ never exceeded 0.87 before annihilation of quartet contamination and were mostly 0.8 at correlated levels of theory. Zero-point vibrational energy (ZPE) corrections have been applied to all optimised structures. Natural Bond Orbital (NBO) analyses were carried out with NBO 5.0[18] linked through the Gaussian 03 program.

Optimized geometries and energies for all transition structures in this study (Gaussian Archive entries) are available as ESI.‡

Results and discussion

Homolytic substitution of acetyl radical with dimethyl sulfide (SMe_2)

We began this study by exploring the chemistry of acetyl radical with dimethyl sulfide. Not only is this the least computationally expensive system in this study, it also provided an opportunity to benchmark various methods before application to the larger systems of interest.

Extensive searching of the C_4H_9SO potential energy surface at all levels of theory employed for optimisation in this study located structure **12** (X = S), of C_s symmetry, as the lowest energy transition state for the reaction of the acetyl radical at the sulfur atom in dimethyl sulfide with expulsion of methyl radical (Scheme 4). The important geometrical features of the transition states **12** (X = S) are summarized in Table 1, while calculated energy barriers ($\Delta E_1^{\ddagger}$ and $\Delta E_2^{\ddagger}$, Scheme 4) together with the corresponding imaginary frequencies are listed in Table 2. Full computational details are available as ESI.‡

Fig. 1 displays the transition state **12** for the attack of the acetyl radical at the sulfur atom in dimethyl sulfide, while Table 1 lists important geometric details for **12** (X = S). Interestingly, the C–S–C attack angles (θ)are predicted to be smaller (less collinear) at the MP2 levels of theory when compared to those obtained at the uncorrelated and DFT levels. For example, at the MP2/aug-cc-pVDZ level of theory, the C–S–C attack angle (θ) is calculated to be 136.5°, compared to 172.4° calculated at the BHandHLYP/aug-cc-pVDZ level of theory.§ The transition state (C–S) separations (r_1) in **12** (X = S) are predicted at all levels of theory to lie in the range:

§ A reviewer suggested that the smaller angles predicted using MP2 may be the result of the use of the frozen core approximation. We can report that virtually identical data are provided by MP2(full); these have been included in the ESI.‡

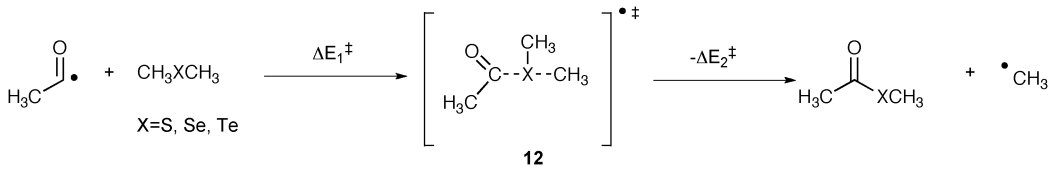

Scheme 4

Table 1 Important calculated geometric features of the transition states **12** (X = S) involved in the reaction of acetyl radical with dimethyl sulfide (Scheme 4, X = S)

Method	r_1/Å	r_2/Å	θ/°
HF/6-311G**	2.136	2.164	172.2
MP2/6-311G*	1.902	2.072	148.5
MP2/cc-pVDZ	1.982	2.066	163.2
MP2/aug-cc-pVDZ	1.872	2.101	136.5
BHandHLYP/6-311G**	2.036	2.107	172.6
BHandHLYP/cc-pVDZ	2.045	2.110	172.9
BHandHLYP/aug-cc-pVDZ	2.040	2.100	172.5
BH3LYP/6-311G**	2.047	2.150	170.7
B3LYP/cc-pVDZ	2.054	2.144	171.3

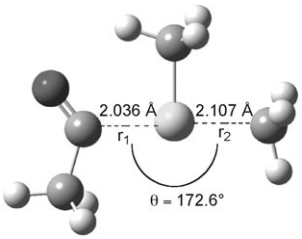

Fig. 1 BHandHLYP/6-311G** optimised structure of transition state **12** (X = S) for the homolytic substitution reaction of acetyl radical with dimethyl sulfide.

1.872–2.136 Å, while the (S–C) distances (r_2) in **12** (X = S) are calculated to be 2.066–2.164 Å. These distances are in the expected ranges when compared with previous calculations of homolytic substitution involving sulfur.[9] Transition state separations are observed to be shorter for the reactions calculated at the correlated levels of theory. At the MP2/aug-cc-pVDZ, the transition state distance r_1 is calculated to be 1.872 Å as compared to 2.040 Å predicted at the BHandHLYP/cc-aug-cc-pVDZ level of theory. Inspection of Table 2 reveals that energy barrier ($\Delta E_1^{\ddagger}$) for the forward reaction (Scheme 4) associated with **12** (X = S) is calculated to be 125.5 kJ mol^{-1} at the HF/6-311G** level of theory. As expected, electron correlation is important in these calculations; MP2/6-311G** serves to lower this energy barrier to 74.4 kJ mol^{-1} for **12** (X = S), while inclusion of zero-point

Table 2 Calculated energy barriers[a] for the forward ($\Delta E_1^{\ddagger}$) and reverse ($\Delta E_2^{\ddagger}$) homolytic substitution reactions of acetyl radical with dimethyl sulfide and imaginary frequencies (ν)[b] of transition states **12** (X = S)

Method	$\Delta E_1^{\ddagger}$	$\Delta E_1^{\ddagger}$ + ZPE	$\Delta E_2^{\ddagger}$	$\Delta E_2^{\ddagger}$ + ZPE	ν
HF/6-311G**	125.5	124.5	131.5	143.0	634i
MP2/6-311G**	74.4	76.9	73.4	86.5	435i
ROMP2/6-311G**//MP2/6-311G**	62.3		57.9		
QCISD/6-311G**//MP2/6-311G**	83.9		77.2		
CCSD(T)/6-311G**//MP2/6-311G**	70.6		66.5		
MP2/cc-pVDZ	73.0	74.5	76.9	89.1	502i
ROMP2/cc-pVDZ//MP2/cc-pVDZ	54.5		54.7		
QCISD/cc-pVDZ//MP2/cc-pVDZ	79.3		77.5		
CCSD(T)/cc-pVDZ//MP2/cc-pVDZ	67.1		68.0		
MP2/aug-cc-pVDZ	55.7	58.1	64.2	76.3	430i
ROMP2/aug-cc-pVDZ//MP2/aug-cc-pVDZ	42.0		47.5		
QCISD/aug-cc-pVDZ//MP2/aug-cc-pVDZ	69.8		71.2		
CCSD(T)/aug-cc-pVDZ//MP2/aug-cc-pVDZ	54.1		59.2		
BHandLYP/6-311G**	76.5	76.8	72.9	83.9	489i
ROMP2/6-311G**//BHandHLYP/6-311G**	60.7		57.9		
QCISD/6-311G**//BHandHLYP/6-311G**	80.6		74.5		
CCSD(T)/6-311G**//BHandHLYP/6-311G**	68.4		59.9		
BHandHLYP/cc-pVDZ	72.0	72.6	72.6	85.7	492i
ROMP2/cc-pVDZ//BHandHLYP/cc-pVDZ	53.9		54.5		
QCISD/cc-pVDZ//BHandHLYP/cc-pVDZ	75.5		74.2		
CCSD(T)/cc-pVDZ//BHandHLYP/cc-pVDZ	63.8		65.1		
BHandHLYP/aug-cc-pVDZ	73.7	74.2	75.5	86.5	486i
ROMP2/aug-cc-pVDZ//BHandHLYP/aug-cc-pVDZ	38.2		44.0		
QCISD/aug-cc-pVDZ//BHandHLYP/aug-cc-pVDZ	66.1		68.3		
CCSD(T)/aug-cc-pVDZ//BHandHLYP/aug-cc-pVDZ	52.4		57.9		
B3LYP/6-311G**	55.3	55.9	49.2	60.3	382i
B3LYP/cc-pVDZ	50.2	50.7	48.4	59.2	391i
QCISD/cc-pVDZ//B3LYP/cc-pVDZ	75.9		73.7		
CCSD(T)/cc-pVDZ//B3LYP/cc-pVDZ	64.2		64.9		

[a] Energies in kJ mol^{-1}. [b] Frequencies in cm^{-1}.

vibrational energy correction (ZPE) has little effect on these barriers. Further improvements in both the basis set quality and levels of correlation provide values of $\Delta E_1^{\ddagger}$ for the reaction involving **12** (X = S) that range from 73.0 kJ mol^{-1} (MP2/cc-pVDZ) to 83.9 kJ mol^{-1} (QCISD/6-311G**//MP2/6-311G**). At the highest level of theory used (CCSD(T)/aug-cc-pVDZ//MP2/aug-cc-pVDZ), energy barriers ($\Delta E_1^{\ddagger}$) of 54.1 kJ mol^{-1} are predicted for the reaction involving **12** (X = S). BHandHLYP/6-311G* and BHandHLYP/cc-pVDZ calculations provide energy barriers ($\Delta E_1^{\ddagger}$) of 76.5 and 72.0 kJ mol^{-1} for the reaction involving **12** (X = S) respectively.

It should be noted that single-point calculations using transition state geometries from either MP2 or DFT methods (θ = 136.5°–172.4°) provide very similar energy barriers, suggesting that the potential energy surface is relatively flat with respect to attack trajectories in that angle range.

It should also be noted that the energy barriers for the forward reaction ($\Delta E_1^{\ddagger}$) and the reverse reaction ($\Delta E_2^{\ddagger}$) are calculated to be 2–15 kJ mol^{-1} lower than those for the homolytic substitution of methyl radical at methanethiol.[9] However, most importantly, the data suggest strongly that the energy barriers calculated for the forward reactions ($\Delta E_1^{\ddagger}$) and the reverse reactions ($\Delta E_2^{\ddagger}$) for the attack of acetyl radicals at the sulfur atom in dimethyl sulfide are very similar and as such suggest that the reaction may be reversible.

Recently, it has been reported that acyl radicals can act as electrophiles through multi-component orbital interactions.[11c,19] With our continued interest in acyl radicals and multi-component orbital interactions in radical chemistry, natural bond orbital (NBO) analyses were performed for transition states **12**; these calculations reveal interesting orbital interactions that are represented pictorially in Fig. 2. Previous studies established that the BHandHLYP/6-311G** method is reliable for the study of acyl and related radical chemistry;[20] accordingly, and for consistency, we chose to perform all our NBO analyses using this method.

As such, NBO analysis for attack of acetyl radical at the sulfur atom in dimethyl sulfide reveals a SOMO → σ^*_{S-C} interaction worth 388 kJ mol^{-1}, which is evident in the α spin-set. Clearly evident in the β spin-set is a strong interaction between the unpaired acetyl radical (SOMO) and the lone pair on sulfur (HOMO). This interaction is calculated to be approximately four times larger than the SOMO → σ^*_{S-C} interaction (LP_S → SOMO is calculated to be 1419 kJ mol^{-1}). It is interesting to note the calculation of a third interaction involving a sulfur lone pair and the π* orbital of the carbonyl π-system. This secondary interaction is apparent in both the α and β spin-sets and is worth 66 kJ mol^{-1}. Clearly these calculations suggest that the acetyl radical is acting predominately as an electrophilic radical in its reaction at the sulfur atom of dimethyl sulfide, with the LP_S → SOMO interaction contributing to 76% of the total orbital interaction. Visualization of the Kohn–Sham orbitals generated at the BHandHLYP/6-311G** level of theory reveals that the secondary interaction (66 kJ mol^{-1}) complements the primary interaction and exists in order to derive maximum energy gain from the available orbitals (Fig. 3).

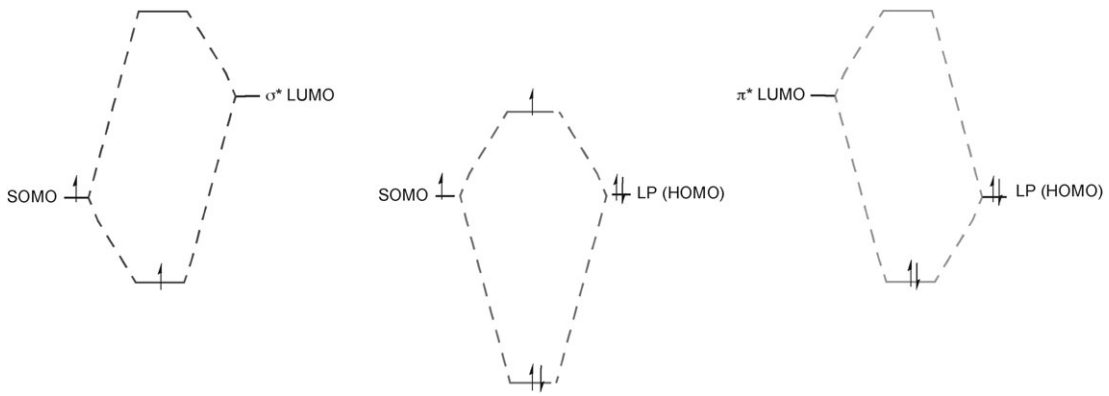

Fig. 2 Orbital interaction diagram for the key bond-forming step involved in the homolytic substitution of acetyl radical at the heteroatom in dimethyl sulfide (transition state **12**, X = S). Similar interactions operate for reaction involving dimethyl selenide and telluride.

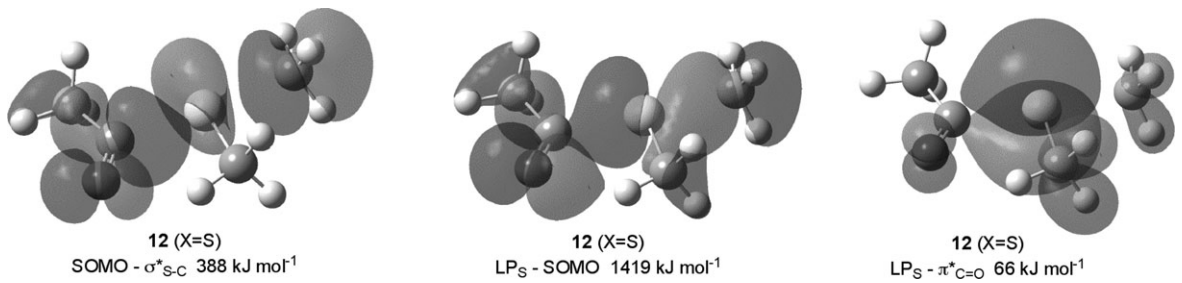

Fig. 3 BHandHLYP/6-311G** generated Kohn–Sham orbital diagrams for transition state **12** (X = S).

Homolytic substitution of acetyl radical with dimethyl selenide ($SeMe_2$) and dimethyl telluride

Calculations for higher heteroatoms such as tellurium are complicated by the lack of availability of reliable all-electron basis sets, as well as the requirement for relativistic correction. Previous benchmarking studies, however, have shown that *ab initio* calculations for homolytic substitution chemistry involving main group higher heteroatoms using double-ζ pseudopotential basis set of Hay and Wadt,[15] supplemented with appropriated *d*-functions,[16] are very similar to those obtained using the 6-311G** basis set (see above).[10b,c,20] With this in mind, we are comfortable in comparing data generated using the DZP basis set for calculations involving tellurium with those generated using 6-311G** for the remaining atoms in this study.

Extensive searching of the C_4H_9XO (X = Se, Te) potential energy surfaces located structures **12** (X = Se, Te) as transition states for the homolytic substitution reactions (Scheme 4) at all levels of theory employed in this study. The important geometrical features of the transition states **12** (X = Se, Te) are summarized in Fig. 4 and Table 3, while the calculated energy barriers ($\Delta E_1^{\ddagger}$ and $\Delta E_2^{\ddagger}$, Scheme 4) together with the corresponding imaginary frequencies are listed in Table 4. Full computational details are available as ESI.‡

In previous calculations,[9,12] results have suggested that homolytic substitution reactions at tellurium are predicted to involve hypervalent intermediates. It is interesting to note that at no level of theory employed in this study could intermediates be located.

Not unexpectedly, transition states **12** (X = Se, Te) bear a striking resemblance to those calculated for the analogous reactions with dimethyl sulfide **12** (X = S). Transition states **12** (X = Se, Te) are also predicted to adopt an almost collinear arrangement, with C_S symmetry, of the attacking acetyl radical and the leaving methyl radical. As can be seen in Fig. 4 and Table 3, the C–X separations (r_1) in **12** are calculated to lie in the range 2.037–2.279 Å and 2.224–2.434 Å for reactions involving dimethyl selenide and dimethyl telluride, respectively, while the X–C distances (r_2) in **12** are predicted to be in the range 2.329 Å (Se) and 2.562Å (Te). As with the reaction involving sulfur, correlated levels of theory once again predict transition state separations that are slightly shorter and slightly less collinear than those calculated for the uncorrelated and DFT methods.§

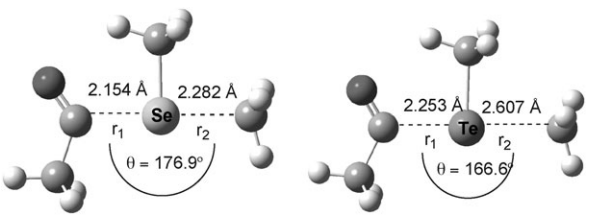

Fig. 4 BHandHLYP/6-311G** (Se) and BHandHYP/DZP (Te) optimized structure of transition states **12** (X = Se, Te) for the substitution reaction of acetyl radicals with dimethyl selenide and dimethyl telluride (Scheme 4, X = Se, Te).

Table 3 Important calculated geometric features[a] of the transition states **12** (X = Se, Te) involved in the reaction of acetyl radical with dimethyl selenide and dimethyl telluride (Scheme 4, X = Se, Te)

	Method	r_1	r_2	θ
Se	HF/6-311G**	2.279	2.329	176.5
	MP2/6-311G*	2.107	2.247	178.3
	MP2/cc-pVDZ	2.093	2.234	168.6
	MP2/aug-cc-pVDZ	2.037	2.242	150.1
	BHandHLYP/6-311G**	2.154	2.282	176.9
	BHandHLYP/cc-pVDZ	2.153	2.276	177.1
	BHandHLYP/aug-cc-pVDZ	2.150	2.266	176.7
Te	HF/DZP	2.434	2.551	178.2
	MP2/DZP	2.224	2.562	159.0
	BHandHLYP/DZP	2.253	2.607	166.6

[a] Distances in Å and angle in degree.

Inspection of Table 4 reveals that the energy barriers ($\Delta E^{\ddagger}$) for the reaction of the acetyl radical with dimethyl selenide are calculated to lie in the range of 29–96 kJ mol^{-1}, while those for the reaction with dimethyl tellurides are calculated to be 29–70 kJ mol^{-1}. As can be seen from the table, all of the energy barriers ($\Delta E_2^{\ddagger}$) for the reverse reactions are always lower than those ($\Delta E_1^{\ddagger}$) for the forward process at all levels of theory, indicating these reactions are predicted to be endothermic. This is not surprising, given the stability of the acetyl radical over the methyl radical.

NBO analyses were performed at the BHandHLYP/6-311G** level of theory on transition states **12** (X = Se) and at the BHandHLYP/DZP level of theory on **12** (X = Te). Visualization of the Kohn–Sham orbitals (available as ESI‡, Fig. S1) depicts the overlap of the two reacting units. For reactions involving **12** (X = Se) the SOMO → σ^*_{Se-C} interaction, calculated to be worth 394 kJ mol^{-1}, is apparent in the α spin-set, with a contribution of 1817 kJ mol^{-1} in the β spin-set from the LP_{Se} → SOMO interaction (Fig. S1, ESI‡). This analysis predicts the LP_{Se} → SOMO interaction to be 4.6 times larger than the SOMO → σ^*_{Se-C} interaction suggesting that the acetyl radical is acting as an electrophile. Once again, apparent in the α and β spin-sets is a third interaction involving a selenium lone pair and the π* orbital and is worth 59 kJ mol^{-1}. Consequently, these data suggest that the acetyl radical is acting as an electrophilic radical in its reaction with dimethyl selenide. NBO analysis for attack of the acetyl radical at the tellurium atom in dimethyl telluride reveals the SOMO → σ^*_{Te-C} interaction to be worth 420 kJ mol^{-1} for transition state **9** (X = Te), evident in the α spin-set, while the LP_{Te} → SOMO interaction, evident in the β spin-set, is calculated to contribute to only 28 kJ mol^{-1}. Clearly, these calculations indicate that, in its reaction with dimethyl telluride, the acetyl radical is observed to act predominantly as a nucleophilic radical, an observation not unexpected, as the tellurium atom is significantly less electronegative than either sulfur or selenium. Of significance is the calculation of a third strong interaction involving the tellurium lone pair and the π* orbital of the carbonyl π-system. This secondary interaction, apparent in both the α and β spin-sets, is worth 121 kJ mol^{-1}.

Effects of alkyl substitution: homolytic substitution reaction of acetyl radical with XMeR (X = S, Se, Te; R = Et, *i*-Pr, *t*-Bu)

As described above, reactions involving selenium and tellurium have been calculated to be endothermic; in other words, acetyl

Table 4 Calculated energy barriers[a] for the forward ($\Delta E_1^{\ddagger}$) and reverse ($\Delta E_2^{\ddagger}$) homolytic substitution reactions of acetyl radical with dimethyl selenide and dimethyl telluride and imaginary frequencies (ν)[b] of transition states **12** (X = Se, Te)

X	Method	$\Delta E_1^{\ddagger}$	$\Delta E_1^{\ddagger}$ + ZPE	$\Delta E_2^{\ddagger}$	$\Delta E_2^{\ddagger}$ + ZPE	ν
Se	HF/6-311G**	95.3	94.1	91.7	103.0	433i
	MP2/6-311G**	55.2	56.0	46.4	57.9	417i
	ROMP2/6-311G**//MP2/6-311G**	48.9		36.8		
	QCISD/6-311G**//MP2/6-311G**	57.0		42.5		
	CCSD(T)/6-311G**//MP2/6-311G**	45.8		34.1		
	MP2/cc-pVDZ	53.1	54.5	48.1	60.1	400i
	ROMP2/cc-pVDZ//MP2/cc-pVDZ	45.6		36.9		
	QCISD/cc-pVDZ//MP2/cc-pVDZ	55.7		45.1		
	CCSD(T)/cc-pVDZ//MP2/cc-pVDZ	44.6		37.0		
	MP2/aug-cc-pVDZ	37.9	38.7	37.8	48.6	337i
	ROMP2/aug-cc-pVDZ//MP2/aug-cc-pVDZ	29.9		26.8		
	QCISD/aug-cc-pVDZ//MP2/aug-cc-pVDZ	46.3		39.3		
	CCSD(T)/aug-cc-pVDZ//MP2/aug-cc-pVDZ	32.5		29.5		
	BHandLYP/6-311G**	53.9	54.1	42.5	54.0	348i
	ROMP2/6-311G**//BHandHLYP/6-311G**	49.6		38.7		
	QCISD/6-311G**//BHandHLYP/6-311G**	55.3		41.2		
	CCSD(T)/6-311G**//BHandHLYP/6-311G**	44.1		32.2		
	BHandHLYP/cc-pVDZ	51.4	51.9	43.3	54.1	347i
	ROMP2/cc-pVDZ//BHandHLYP/cc-pVDZ	47.6		40.8		
	QCISD/cc-pVDZ//BHandHLYP/cc-pVDZ	53.1		44.0		
	CCSD(T)/cc-pVDZ//BHandHLYP/cc-pVDZ	42.3		36.5		
	BHandHLYP/aug-cc-pVDZ	53.1	53.0	45.0	54.7	346i
	ROMP2/aug-cc-pVDZ//BHandHLYP/aug-cc-pVDZ	31.9		29.4		
	QCISD/aug-cc-pVDZ//BHandHLYP/aug-cc-pVDZ	42.4		35.9		
	CCSD(T)/aug-cc-pVDZ//BHandHLYP/aug-cc-pVDZ	29.5		27.1		
Te	HF/DZP	69.7	68.5	49.8	60.6	327i
	MP2/DZP	38.9	39.5	18.8	29.2	289i
	ROMP2/DZP//MP2/DZP	42.8		19.4		
	QCISD/DZP//MP2/DZP	39.0		13.4		
	CCSD(T)/DZP//MP2/DZP	29.2		7.4		
	BHandHLYP/DZP	35.5	34.9	10.8	20.0	218i
	ROMP2/DZP//MP2/DZP	38.3		11.8		
	QCISD/DZP//BHandHLYP/DZP	38.2		13.1		
	CCSD(T)/DZP//BHandHLYP/DZP	29.0		7.4		

[a] Energies in kJ mol^{-1}. [b] Frequencies in cm^{-1}.

radicals prefer to be the leaving group rather than the attacking species, while reactions involving sulfur show no preference for the acetyl radical acting as either the leaving group or the attacking radical. In order to further explore the factors that effect this chemistry, we briefly examined the effects of alkyl substitution on the reactions in question. Accordingly, the reactions of acetyl radicals with alkylmethyl sulfide, -selenide and -telluride (H_3CXR), in which ethyl, isopropyl and *tert*-butyl radicals were chosen as the leaving groups, were modelled. Because of the significant increase in computational size and given the BHandHLYP method performs well in the above-mentioned work, the reaction profiles described in Scheme 4 were examined using this method. Thus, extensive searching of the CH_3COXCH_3R (X = S, Se, Te; R = Et, *i*-Pr, *t*-Bu) potential energy surface at the BHandHLYP/6-11G** (S, Se) or BHandHLYP/DZP (Te) levels of theory located structures **13** as transition states in the homolytic substitution reactions of interest (Scheme 5). The important geometrical features of these structures are summarized in Table 5, and the calculated energy barriers are listed in Table 6. Full structural details are available as ESI.‡

Not unexpectedly, transition states **13** (X = S, Se, Te; R = Et, *i*-Pr, *t*-Bu) are calculated to have similar structures to the analogous reactions involving **12** (X = S, Se, Te). Again, transition states are predicted to adopt an almost collinear arrangement with C_s symmetry. As shown in Table 5, C–X distances (r_1) in **13** are calculated to lie between 2.062 Å (X = S, R = Et) and 2.438 Å (X = Te, R = *t*-Bu) at the level of theory employed, while X–C separations (r_2) in **13** are predicted to be between 2.100 Å (X = S, R = Et) and 2.438 Å (X = Te, R = *t*-Bu). Interestingly, while the calculated bond distances for the substitution reactions involving sulfur and selenium (r_1 and r_2) and tellurium (r_1) generally increase in the order of methyl < ethyl < isopropyl < *tert*-butyl, r_2 separations in **12** predicted in the transition states involving tellurium decrease in the same order of the leaving radical.

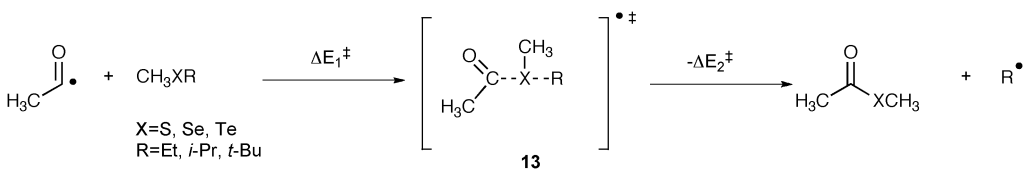

Scheme 5

Table 5 Important BHandHLYP/6-311G** (DZP) calculated geometric features of the transition states **13** (X = S, Se, Te; R = Et, *i*-Pr, *t*-Bu)

X	R	Method	r_1/Å	r_2/Å	θ/°
S	Et	BHandHLYP/6-311G**	2.062	2.100	172.9
	i-Pr	BHandHLYP/6-311G**	2.101	2.117	170.1
	t-Bu	BHandHLYP/6-311G**	2.136	2.121	169.1
Se	Et	BHandHLYP/6-311G**	2.191	2.255	177.3
	i-Pr	BHandHLYP/6-311G**	2.236	2.261	174.8
	t-Bu	BHandHLYP/6-311G**	2.275	2.257	173.6
Te	Et	BHandHLYP/DZP	2.305	2.498	169.5
	i-Pr	BHandHLYP/DZP	2.377	2.452	179.1
	t-Bu	BHandHLYP/DZP	2.438	2.421	179.5

Table 6 BHandHLYP/6-311G** (DZP) calculated energy barriers[a] for the forward ($\Delta E_1^{\ddagger}$) and reverse ($\Delta E_2^{\ddagger}$) homolytic substitution reactions of acetyl radical with ethyl methyl sulfide, isopropyl methyl sulfide, *tert*-butyl methyl sulfide, ethyl methyl selenide, isopropyl methyl selenide, *tert*-butyl methyl selenide, ethyl methyl telluride, isopropyl methyl telluride, and *tert*-butyl methyl telluride, and imaginary frequencies (ν)[b] of transition states **13** (X = S, Se, Te; R = Et, *i*-Pr, *t*-Bu)

X	R	$\Delta E_1^{\ddagger}$	$\Delta E_1^{\ddagger}$ + ZPE	$\Delta E_2^{\ddagger}$	$\Delta E_2^{\ddagger}$ + ZPE	ν
S	Et	70.9	71.5	77.0	85.9	488i
S	*i*-Pr	69.0	70.1	88.8	97.0	496i
S	*t*-Bu	60.2	62.7	94.3	100.1	492i
Se	Et	47.0	47.7	47.7	57.2	342i
Se	*i*-Pr	43.8	45.2	58.6	67.3	349i
Se	*t*-Bu	37.0	38.8	64.4	71.0	331i
Te	Et	23.8	24.4	15.6	23.8	226i
Te	*i*-Pr	17.9	18.2	24.7	31.9	221i
Te	*t*-Bu	11.4	13.2	33.3	39.1	227i

[a] Energies in kJ mol^{-1}. [b] Frequencies in cm^{-1}.

As has been previously reported,[11c,21] the calculated energy barriers ($\Delta E_1^{\ddagger}$) for the forward reaction decrease in the order of methyl > ethyl > isopropyl > *tert*-butyl, while those ($\Delta E_2^{\ddagger}$) for the reverse process increase in the same order of leaving radical. As a result homolytic substitution at the chalcogen atom with expulsion of ethyl, isopropyl and *tert*-butyl groups are predicted to be exothermic, while the expulsion of methyl group is predicted to be endothermic.

Conclusion

In conclusion, *ab initio* and DFT calculations predict that homolytic substitution reactions of acetyl radicals at the heteroatom in dimethyl sulfide, dimethyl selenide and dimethyl telluride with the expulsion of methyl radical proceed *via* smooth transition states and without the involvement of hypervalent intermediates. The data provided suggest that while the reaction of the acetyl radical at the sulfur in dimethyl sulfide is reversible, the analogous reactions involving dimethyl selenide and dimethyl telluride are predicted to be endothermic at all levels of theory employed. However, when the stability of the leaving radical is increased, the reactions in question become exothermic.

Acknowledgements

This work would not have been possible without the generous support of the Australian Research council through the Centers of Excellence Program. We also gratefully acknowledge the support of the Victorian Institute for Chemical Sciences High performance Computing facility and the Australian Partnership for Advanced Computing.

Notes and references

1 For leading reviews, see: (*a*) J. C. Walton, *Acc. Chem. Res.*, 1998, **31**, 99; (*b*) C. H. Schiesser and L. M. Wild, *Tetrahedron*, 1996, **52**, 13265; (*c*) J.-M. Saveant, *Tetrahedron*, 1994, **50**, 10117; (*d*) A. L. J. Beckwith, *Chem. Soc. Rev.*, 1993, **22**, 143; (*e*) R. A. Rossi and S. M. Palacios, *Tetrahedron*, 1993, **49**, 4485.
2 For some reports, see: (*a*) C. A. G. Carter, G. Greidanus, J.-X. Chen and J. M. Stryker, *J. Am. Chem. Soc.*, 2001, **123**, 8872; (*b*) A. M. Stolzenberg and Y. Cao, *J. Am. Chem. Soc.*, 2001, **123**, 9078; (*c*) S. E. Tichy, K. K. Thoen, J. M. Price, J. J. Ferra, Jr., C. J. Petucci and H. I. Kenttaemaa, *J. Org. Chem.*, 2001, **66**, 2726; (*d*) N. Al-Maharik, L. Engman, J. Malmström and C. H. Schiesser, *J. Org. Chem.*, 2001, **66**, 6286; (*e*) S.-K. Kang, H.-W. Seo and Y.-H. Ha, *Synthesis*, 2001, 1321; (*f*) M.-J. Bourgeois, M. Vialemaringe, M. Campahnole and E. Mountaudon, *Can. J. Chem.*, 2001, **79**, 257; (*g*) M. W. Carland, R. L. Martin and C. H. Schiesser, *Tetrahedron Lett.*, 2001, **42**, 4737; (*h*) J. B. Miller and J. R. Salvador, *J. Org. Chem.*, 2002, **67**, 435; (*i*) P. Lightfoot, P. Pareschi and J. C. Walton, *J. Chem. Soc., Perkin Trans. 2*, 2002, 918; (*j*) L. Benati, R. Leardini, M. Minozzi, D. Nanni, P. Spagnolo, S. Strazzari and G. Zanardi, *Org. Lett.*, 2002, **4**, 3079; (*k*) J. Hartung, T. Gottwald and K. Spehar, *Synthesis*, 2002, 1469.
3 (*a*) R. Leardini, G. F. Pedulli, A. Tundo and G. Zanardi, *J. Chem. Soc., Chem. Commun.*, 1985, 1390; (*b*) R. L. Grange, J. Ziogas, A. J. North, J. A. Angus and C. H. Schiesser, *Bioorg. Med. Chem. Lett.*, 2008, **18**, 1241; (*c*) L. Engman, M. J. Laws, J. Malmström, C. H. Schiesser and L. M. Zugaro, *J. Org. Chem.*, 1999, **64**, 6764.
4 (*a*) I. Ryu, T. Okuda, K. Nagahara, N. Kambe, M. Komatsu and N. Sonoda, *J. Org. Chem.*, 1997, **62**, 7550; For leading reviews on acyl radicals see: (*b*) C. Chatgilialoglu, D. Crich, M. Komatsu and I. Ryu, *Chem. Rev.*, 1999, **99**, 1991; (*c*) I. Ryu and N. Sonoda, *Angew. Chem., Int. Ed. Engl.*, 1996, **35**, 1050.
5 I. Ryu, T. Okuda, K. Nagahara, N. Kambe, M. Komatsu and N. Sonoda, *J. Org. Chem.*, 1997, **62**, 7550.
6 A. L. J. Beckwith, *Chem. Soc. Rev.*, 1993, **22**, 143.
7 J. A. Franz, D. H. Roberts and K. F. Ferris, *J. Org. Chem.*, 1987, **52**, 2256.
8 (*a*) C. H. Schiesser and L. M. Wild, *Aust. J. Chem.*, 1995, **48**, 175; See also: (*b*) J. M. Howell and J. F. Olsen, *J. Am. Chem. Soc.*, 1976, **98**, 7119; (*c*) C. J. Crammer, *J. Am. Chem. Soc.*, 1990, **112**, 7965; (*d*) C. J. Crammer, *J. Am. Chem. Soc.*, 1991, **113**, 2439.
9 C. H. Schiesser and B. A. Smart, *Tetrahedron*, 1995, **51**, 6051.
10 (*a*) C. H. Schiesser, B. A. Smart and T.-A. Tran, *Tetrahedron*, 1995, **51**, 3327; (*b*) C. H. Schiesser and L. M. Wild, *J. Org. Chem.*, 1998, **63**, 670; (*c*) C. H. Schiesser, M. L. Styles and M. L. M. Wild, *J. Chem. Soc., Perkin Trans. 2*, 1996, 2257; (*d*) C. H. Schiesser and M. L. Styles, *J. Chem. Soc., Perkin Trans. 2*, 1997, 2335.
11 (*a*) C. H. Schiesser, *Chem. Commun.*, 2006, 4055, and references cited therein; (*b*) H. Matsubara, I. Ryu and C. H. Schiesser, *Org. Biomol. Chem.*, 2007, **5**, 3320; (*c*) S. M. Horvat and C. H. Schiesser, *Organometallics*, 2009, **28**, 3311.
12 C. H. Schiesser and L. M. Wild, *J. Org. Chem.*, 1999, **64**, 1131.
13 M. J. Frisch, G. W. Trucks, H. B. Schlegel, G. E. Scuseria, M. A. Robb, J. R. Cheeseman, J. A. Montgomery, T. Vreven, Jr., K. N. Kudin, J. C. Burant, J. M. Millam, S. S. Iyengar, J. Tomasi, V. Borone, B. Mennucci, M. Cossi, G. Scalmani, N. Rega, G. A. Peterson, H. Nakatsuji, M. Hada, M. Ehara, K. Toyota, R. Fukuda, J. Hasegawa, M. Ishida, T. Nakajima, Y. Honda, O. Kitao, H. Nakai, M. Klene, X. Li, J. E. Knox, H. P. Hratchian, J. B. Cross, V. Bakken, C. Adamo, J. Jaramillo, R. Gomperts, R. E. Stratmann, O. Yazyev, A. J. Austin, R. Cammi, C. Pomelli, J. Ochterski, P. Y. Ayala, K. Morokuma, G. A. Voth, P. Salvador, J. J. Dannenberg, V. G. Zakrzewski, S. Dapprich, A. D. Daniels, M. C. Strain, O. Farkas, D. K. Malick, A. D. Rabuck, K. Raghavachari, J. B. Foresman, J. V. Ortiz, Q. Cui, A. G. Baboul, S. Clifford, J. Cioslowski,

B. B. Stefanov, G. Liu, A. Liashenko, P. Piskorz, I. Komaromi, R. L. Martin, D. J. Fox, T. Keith, M. A. Al-Laham, C. Y. Peng, A. Nanayakkara, M. Challacombe, P. M. W. Gill, B. G. Johnson, W. Chen, M. W. Wong, C. Gonzalez and J. A. Pople, *GAUSSIAN 03, Revision B. 05*, Gaussian Inc., Pittsburgh, PA, 2003.
14 W. J. Hehre, L. Radom, P. v. R. Schleyer and P. A. Pople, *Ab initio Molecular Orbital Theory*, Wiley, New York, 1986.
15 (*a*) W. R. Wadt and P. J. Hay, *J. Chem. Phys.*, 1985, **82**, 284; (*b*) P. J. Hay and W. R. Wadt, *J. Chem. Phys.*, 1985, **82**, 270; (*c*) P. J. Hay and W. R. Wadt, *J. Chem. Phys.*, 1985, **82**, 299.
16 B. A. Smart, PhD thesis, The University of Melbourne, 1994.
17 T. H. Dunning and P. J. Hay, *Modern Theoretical Chemistry*, Plenum, New York, 1976, ch. 1, pp. 1–28.
18 E. D. Glendening, J. K. Badenhoop, A. E. Reed, J. E. Carpenter, J. A. Bohmann, C. M. Morales and F. Weinhold, *NBO 5.0*, Theoretical Chemical Institute, University of Wisconsin, Madison WI, 2001.
19 (*a*) C. H. Schiesser, U. Wille, H. Matsubara and I. Ryu, *Acc. Chem. Res.*, 2007, **40**, 303, and references cited therein; (*b*) S. Kyne, S. C. Schiesser and H. Matsubara, *J. Org. Chem.*, 2008, **73**, 427; (*c*) E. H. Krenske and C. H. Schiesser, *Org. Biomol. Chem.*, 2008, **6**, 854; (*d*) S. Kyne and S. H. Schiesser, *Aust. J. Chem.*, 2009, **62**, 728.
20 S. M. Horvat and C. H. Schiesser, *Organometallics*, 2000, **19**, 1239.
21 S. Lobachevsky, C. H. Schiesser, C. Y. Lin and M. L. Coote, *J. Phys. Chem. A*, 2008, **112**, 13622.